Aquatic Mammals 2025, *51*(6), 464-481, DOI https://doi.org/10.1578/AM.51.6.2025.464

RGB and Multispectral UAV Mapping of Dugong Foraging Hotspots and Seagrass Beds in Thailand and Mozambique

Janmanee Panyawai,[1, 2, 3] Milica Stankovic,[2, 3] Eduardo Infantes,[4] Damboia Cossa,[5, 6] Kanyanat Kaewutai,[2] and Anchana Prathep[1, 2, 3]

[1]*Division of Biological Science, Faculty of Science, Prince of Songkla University, Hat Yai, Songkhla, 90112 Thailand*
[2]*Excellence Center for Biodiversity of Peninsular Thailand, Faculty of Science, Prince of Songkla University, Hat Yai, Songkhla, 90112 Thailand*
[3]*Dugong and Seagrass Research Station, Prince of Songkla University, Hat Yai, Songkhla, 90112 Thailand*
E-mail: anchana.p@psu.ac.th
[4]*Department of Biological and Environmental Sciences, University of Gothenburg, Kristineberg, Sweden*
[5]*Department of Marine Sciences, University of Gothenburg, Kristineberg, Sweden*
[6]*Department of Biological Sciences, Eduardo Mondlane University, Maputo, Mozambique*

Abstract

Unmanned aerial vehicles (UAVs) are widely used for mapping and monitoring coastal ecosystems due to their high accuracy and efficiency, providing surveys that are less costly and time-consuming compared to vessel-based methods. This study demonstrates the utility of using UAV imagery combined with ground surveys to evaluate the spatial distribution of dugong (*Dugong dugon*) foraging based on their feeding trails and associated intertidal seagrass beds in (1) Dugong Tower and (2) Juhoi, Libong Island, Thailand, and (3) Saco, Inhaca Island, Mozambique, as well as the temporal distribution of dugong feeding trails on Mook Island, Thailand. Ground survey results showed that small- and medium-sized seagrass species are the most preferred by dugongs. RGB images capture detailed plant characteristics, while NDVI images assess vegetation density, with higher values indicating denser vegetation. In denser areas (e.g., Juhoi), both images detected feeding trails, with RGB identifying distinct trails and NDVI highlighting contrasts. In sparse areas (e.g., Dugong Tower and Saco), NDVI provided clearer detection. However, UAVs may be limited by restricted flight endurance and sea state conditions, as well as by water level, turbidity, and sun glint. This study highlights the potential of drones to survey and monitor dugong populations indirectly, assisting coastal managers in assessing seagrass availability for dugongs and observing dugong behavior in their natural habitat, particularly in hotspot areas.

Key Words: aerial survey, dugong feeding trails, environmental mapping, seagrasses, UAVs

Introduction

Unmanned aerial vehicles (UAVs), also known as drones, are increasingly being utilized to expedite ground-based observations, significantly reducing time and labor compared to vessel- or airplane-based surveys. The prevailing trend in research is to favor multirotors, primarily due to their straightforward control mechanisms and accurate positioning capabilities. Additionally, the cost-effectiveness of UAV monitoring stands out as a viable option when contrasted with observation techniques involving airplanes or helicopters (Schofield et al., 2019). Within the field of aquatic wildlife science, UAVs play various roles, including monitoring the abundance of animals (Cleguer et al., 2021), conducting population assessments (Hodgson et al., 2013), making individual identifications (Ryan et al., 2022), evaluating body size and condition (Infantes et al., 2022; Ramos et al., 2022; Carroll et al., 2024), and mapping habitat (Cossa et al., 2023). UAVs are being deployed to elucidate several aspects of dugong ecology, biology, and behavior (Infantes et al., 2020), particularly in estimating the abundance of dugongs (Raoult et al., 2020). Due to the elusive behavior of dugongs (*Dugong dugon*), accurately determining the sizes of individual populations is challenging.

Dugong feeding trails are formed when dugongs graze up seagrasses, including their roots, leaving a shallow, meandering track of about equal width and

depth (Preen, 1995). The feeding trails can be used as an indicator of their feeding ground utilization (Marsh et al., 2011). The recovery of seagrass following disturbances caused by dugong herbivory was estimated to be relatively rapid for *Halophila ovalis*, occurring in less than 20 d (Nakaoka & Aioi, 1999). In contrast, other seagrass species, such as *Cymodocea* spp. and *Thalassia* spp., may take longer to recover due to their slower growth rates and differences in resilience (Kilminster et al., 2015). Recovery times can also be influenced by environmental factors, including water quality, sediment stability, and grazing intensity. However, tracking dugong feeding trails is a method that indirectly monitors their presence and feeding activity, which could contribute to conservation and management. Moreover, these trails can be geolocated and mapped out for pattern analysis.

Monitoring the distribution of dugong feeding trails in intertidal seagrass areas has been proven to be an effective approach for observing detailed dugong feeding behavior. As dugongs uproot entire plants, the leaves, rhizomes, and roots of seagrasses become exposed along the edges of their feeding trails (Marsh et al., 2011). These trails serve as direct evidence of feeding activity and provide crucial data on feeding location, seagrass consumption, and feeding direction (Budiarsa et al., 2021). In traditional techniques, researchers target areas within seagrass meadows—a unified ecological habitat characterized by continuous or semi-continuous seagrass, often comprising one or more species—along transects to gather information on seagrass. For instance, the species and percent coverage of grazed seagrass are determined by assessing the seagrass composition along the observed dugong feeding trails and measuring the width and length of the trails (Preen, 1995; Yamamuro & Chirapart, 2005; Budiarsa et al., 2021). However, these methods consume a lot of manpower and time, covering only a small area of the intertidal seagrass meadow due to time and tide constraints (Murfitt et al., 2017).

In recent years, there has been a rise in the utilization of UAVs as an affordable and effective monitoring solution in various contexts. The use of UAVs has demonstrated their utility in assessing the presence or absence of seagrass cover (Duffy et al., 2018b; Price et al., 2022) and in differentiating seagrass species (Hamad et al., 2022; Tahara et al., 2022; Karang et al., 2024). Additionally, some studies have attempted to discriminate seagrass species from seaweed (Román et al., 2021), coral, and unvegetated areas such as rock and bare sediment (Nababan et al., 2021; Riniatsih et al., 2021). Nevertheless, there are few methods using UAVs to observe dugong feeding trails. Yamato et al. (2021) used deep neural networks-based automated extraction to detect changes in position from UAV images and to identify dugong feeding trails in intertidal seagrass beds. Meanwhile, Cossa et al. (2023) employed UAVs and machine-learning techniques to monitor dugong feeding grounds and evaluate the influence of gillnet fishing activities on these areas. Therefore, some researchers have monitored and mapped seagrass and dugong feeding trail distributions in intertidal zones, providing important information for the conservation and management of seagrass habitats in coastal zones.

In this study, we present a cost-effective aerial survey approach for identifying dugong feeding grounds in intertidal seagrass meadows. We also provide examples of seagrass classification schemes. Additionally, we combine this aerial survey information with ground surveys to obtain estimates of meadow area and the distribution of dugong feeding trails in Libong Island and Mook Island in southern Thailand, as well as in Inhaca Island in southern Mozambique.

Methods

Study Site and Data Acquisition

Our study involves a spatial assessment conducted across three distinct areas: (1) Dugong Tower and (2) Juhoi in Libong Island, Trang, Thailand (Figure 1A), and (3) Saco, Inhaca Island, Mozambique (Figure 1B). We also conducted a temporal assessment within one area in Mook Island, Trang Province, Thailand (Figure 1A).

For the spatial assessment of dugong feeding trails study, the imagery was obtained from three study sites: (1) Dugong Tower and (2) Juhoi in Libong Island, Trang, Thailand, during a comprehensive survey of dugong reproductive behavior conducted around the island in February 2019 and February 2020 (Infantes et al., 2020; Figure 1A; Table 1), and (3) Saco, Inhaca Island, Mozambique, as reported by Cossa et al. (2023; Figure 1B; Table 1). The percent seagrass coverage in Libong Island ranged from 20 to 40%, with six identified species: *Enhalus acoroides*, *Cymodocea rotundata*, *Halophila ovalis*, *Halodule pinifolia*, *Halodule uninervis*, and *Thalassia hemprichii*. Seagrass meadows at Inhaca Island cover approximately 50% of the intertidal areas around the island with nine identified species: *C. rotundata*, *Oceana serrulata* (formerly *C. serrulata*), *H. ovalis*, *H. uninervis*, *T. hemprichii*, *Thalassodendron ciliatum*, *Thalassodendron leptocule*, *Syringodium isoetifolium*, and *Zostera capensis* (Bandeira & Gullström, 2014). The aerial surveys for these studies were conducted at an altitude of 80 m in

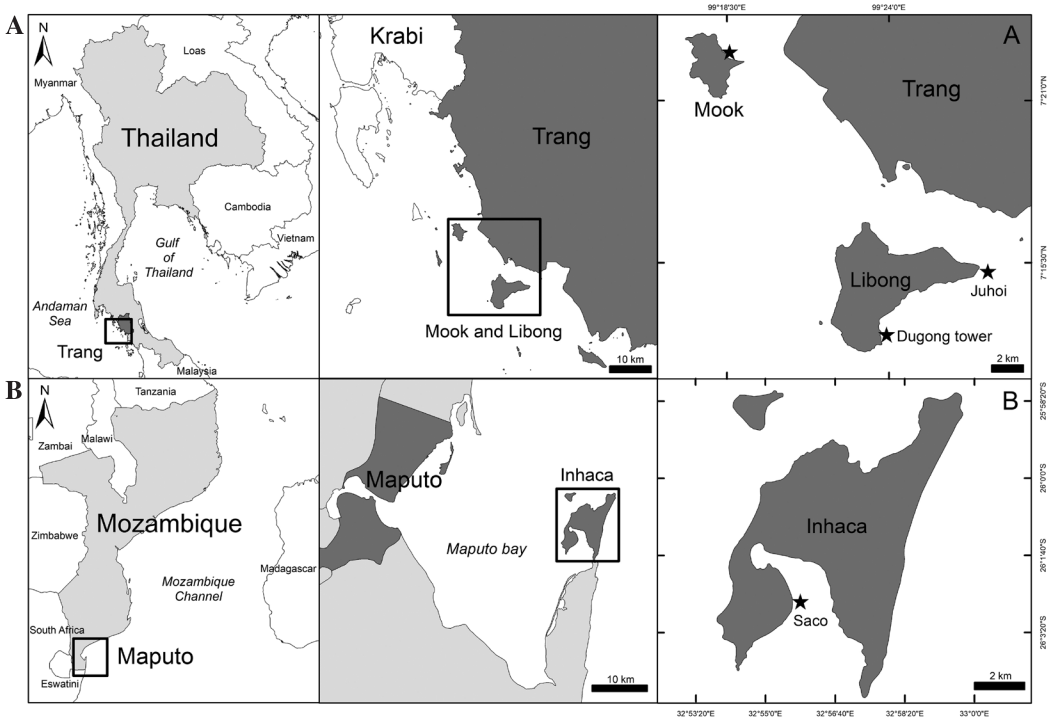

Figure 1. Map of the study sites (shown as stars) in (A) Mook Island and Libong Island (including the two sites: Dugong Tower and Juhoi), Trang Province, Southern Thailand, and (B) Saco, Inhaca Island, Maputo Province, Southern Mozambique

Table 1. Drone flight information

Image used	Sites	Date (d/mo/y)	Seasons	Area cover (km^2)	Camera model	Resolution (cm $pixel^{-1}$)	No. of images	Flight time (min)
Spatial assessment	Dugong Tower	24/2/2020	Dry	0.10	RGB	2.18	194	18
		24/2/2020		0.14	Multispectral	5.56	274	15
	Juhoi	26/2/2020	Dry	0.16	RGB	2.18	229	15
		26/2/2020		0.35	Multispectral	5.56	688	42
	Saco	19/11/2018	Wet	0.15	RGB	2.18	298	18
		19/11/2018		0.10	Multispectral	5.56	199	11
Temporal assessment	Mook Island	2/7/2020	Wet	0.24	RGB	2.18	454	31
		18/8/2020		0.44		2.18	837	62
		13/11/2020		0.24		2.18	453	26
		16/12/2020	Dry	0.20		2.18	380	23
		12/2/2021		0.14		2.18	275	17
		14/3/2021		0.29		2.18	558	35
		10/4/2021		0.20		2.18	366	22

the intertidal zone during the lowest tide of each study site (Table 1). The UAV was flown in regular transects in pre-programmed flights using *pix-4DCapture* or *DroneDeploy*® software, a survey planning software for drone mapping, covering the entire area. The front and side image overlaps were set to 80 and 60%, respectively. The visible (RGB) imagery was obtained using a quadcopter drone (Phantom 4 Pro, Version 2.0; DJI, Nanshan, Shenzhen, China) with RGB camera models, and the multispectral imagery was conducted using a multispectral camera (Micasense; Red Edge, Arlington, VA, USA) on a quadcopter drone (Matrice 200, DJI) (Table 1). Ground-truth observations were conducted concurrently with the aerial surveys to collect spatially referenced data on seagrass meadows using a modified spot-check methodology (McKenzie, 2006). A total of 30 to 50 observations were recorded, including geographic coordinates (latitude and longitude), seagrass species, and percentage cover. Geographic coordinates were recorded as waypoints utilizing Garmin GPSMap eTrex 30 devices, achieving positional accuracy of ±5 m. Seagrass species and cover percentage were assessed within 50 × 50 cm quadrats. These ground-truth observations were later compared with the UAV orthomosaic through manual visual interpretation (Trinh et al., 2023). The field data provided foundational training data for the UAV orthomosaic classification.

To examine the temporal assessment of dugong feeding trails, ground-truth data and imagery were obtained from July 2020 to April 2021 at Mook Island, Trang Province, Thailand (Figure 1A; Table 1). The percentage cover of seagrass in the area ranged from 17 to 34%, with six identified species identified: *E. acoroides*, *C. rotundata*, *H. ovalis*, *H. pinifolia*, *H. uninervis*, and *T. hemprichii*. UAV flights were performed, covering approximately 0.39 km^2 in the northeast intertidal seagrass meadows of Mook Island during low tide (Table 1). To ensure consistency, the flights were conducted using the same method as the RGB imagery for the spatial assessment. The ground-truth observations were conducted during the spring tide period when the intertidal seagrass beds were exposed to air. Five hundred 50 × 50 cm quadrats were placed in 15 m intervals from each other in the study area, covering a total area of around 0.115 km^2. The ground positioning of each quadrat was marked using waypoints on a handheld Garmin GPSMap eTrex 30 placed at the center of each quadrant. Subsequently, the species and percentage cover of seagrass within the quadrats were recorded following standard Seagrass-Watch protocols (McKenzie, 2006).

Image Processing and Identification of Dugong Feeding Trails

All the images were processed using the Agisoft PhotoScan (Agisoft LLC, St. Petersburg, Russia) to generate orthomosaics (aerial maps) of the study areas. RGB color orthomosaics were generated from red (R), green (G), and blue (B) bands. The multispectral orthomosaics were built for each of the five bands (R, G, B, near-infrared [NIR], and Red Edge). The process included alignment, optimization, Digital Elevation Model (DEM), and orthomosaic building, and then separating orthomosaics per band by using the raster calculator. Normalized Difference Vegetation Index (NDVI) maps were generated from R and NIR bands. NDVI is specifically designed to highlight variations in vegetation health. It calculates the difference between NIR and R reflectance, emphasizing the presence and condition of vegetation (Chen et al., 2021; Huang et al., 2021). The NDVI formula can be expressed as follows (Li et al., 2023):

$$\mathrm{NDVI} = \frac{NIR-R}{NIR+R} \quad (1)$$

NDVI varies between -1 to +1. The higher values suggest healthy vegetation (NIR > R, a value close to +1), lower values indicate bare soil or stressed vegetation (R > NIR, a value close to -1), and values near 0 represent neutral or mixed areas (NIR ≈ R) (Figure S1; the supplemental figures for this article are available on the *Aquatic Mammals* website).

The comparison between RGB and NDVI highlights two key insights: (1) differences in vegetation characteristics and density, and (2) feeding trail detection. RGB images provide detailed information on plant characteristics, such as color variations that may indicate species, while NDVI images are better suited for assessing vegetative density.

Dugong feeding trails can be identified generally as sinuous paths of clear substrate through patches of seagrass. Their width is recognizable as being between 9 to 30 cm (Adulyanukosol et al., n.d.; Shawky, 2019; Tsutsumi et al., 2000). The dugong feeding trails were quite different from other features found in seagrass such as boat propeller scars or boring by other animals (Figure S2). In this study, only dugong feeding trails that clearly occurred within seagrass meadows were used in the analysis.

The spatial assessment of dugong feeding trails was conducted on orthomosaics at three locations—(1) Dugong Tower and (2) Juhoi in Libong Island, Trang, Thailand, and (3) Saco, Inhaca Island, Mozambique—using *QGIS*, Version 3.28.3 (QGIS Development Team, 2023), for both RGB

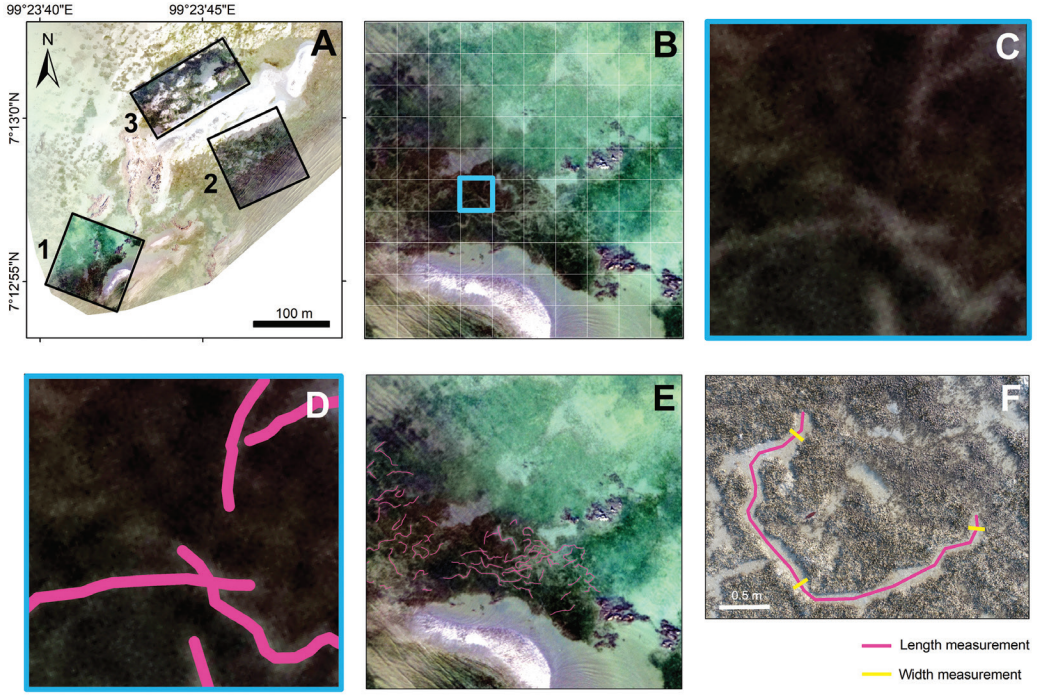

Figure 2. The identification of dugong (*Dugong dugon*) feeding trails for spatial assessment: (A) example of the three targeted sampling areas (1 ha), numbered 1 to 3; (B) zooming to the targeted sampling area 1, with 10 × 10 m grid template and template applied to mosaic ready for assessment (blue square indicates the cell shown in C and D); (C) zooming to one 10 × 10 m cell; (D) manually drawing lines along the dugong feeding trails (line layer); (E) the trail abundance in sampling area 1; and (F) example of the length and width measurement.

and NDVI maps. Three targeted sampling areas (10,000 m^2, 1 ha) were randomly created in the hotspot of the dugong feeding trail in each site; these excluded obvious vegetated land areas and deep water (Figure 2A). A fixed grid template with 10 × 10 m cells was created to overlay on the targeted sampling area (Figure 2B). Each individual grid cell (10 × 10 m; Figure 2C) was assessed by the Seaweed and Seagrass Research Unit (SSRU) staff with experience in locating dugong feeding trails in the field. For the assessment, SSRU staff manually drew a line following the trails shown on an LCD computer monitor at a scale of 1:300 or less (Figure 2D), and then repeated the process of drawing a line in every grid cell. The line layers representing the dugong feeding trails in the sampling area (Figure 2E) were used to estimate the length, average width, and area.

The length (m), average width (m), and area (m^2) of dugong feeding trails in each targeted sampling area were estimated using the *QGIS*, Version 3.28.3 (QGIS Development Team, 2023). The length of the feeding trails was calculated from the line layer using the 'Geometry' function and the '$length' expression in the Field Calculator; the average width of the feeding trails (W_i: The average width at each targeted sampling area *i*) was manually measured on the images three times for each of the 30 randomly selected trails (Figure 2F) by using the program measure tools; and the area of the feeding trails was calculated from the line layer using the 'Geometry' function and the '$length * W_i' expression in the Field Calculator.

The temporal assessment of dugong feeding trails was conducted on RGB orthomosaics from Mook Island, Trang Province, Thailand, using *QGIS*, Version 3.28.3 (QGIS Development Team, 2023). A fixed grid template with 100 × 100 m cells was created to overlay on the sampling area (Figure 3A). Each individual grid cell (100 × 100 m) was assessed by SSRU staff with experience in locating dugong feeding trails in the field. For the assessment, SSRU manually drew a line following the trails shown on an LCD computer monitor at a scale of 1:300 or less (Figure 3B & C), and again repeated the process of drawing a line in every grid cell. The line layer representing dugong

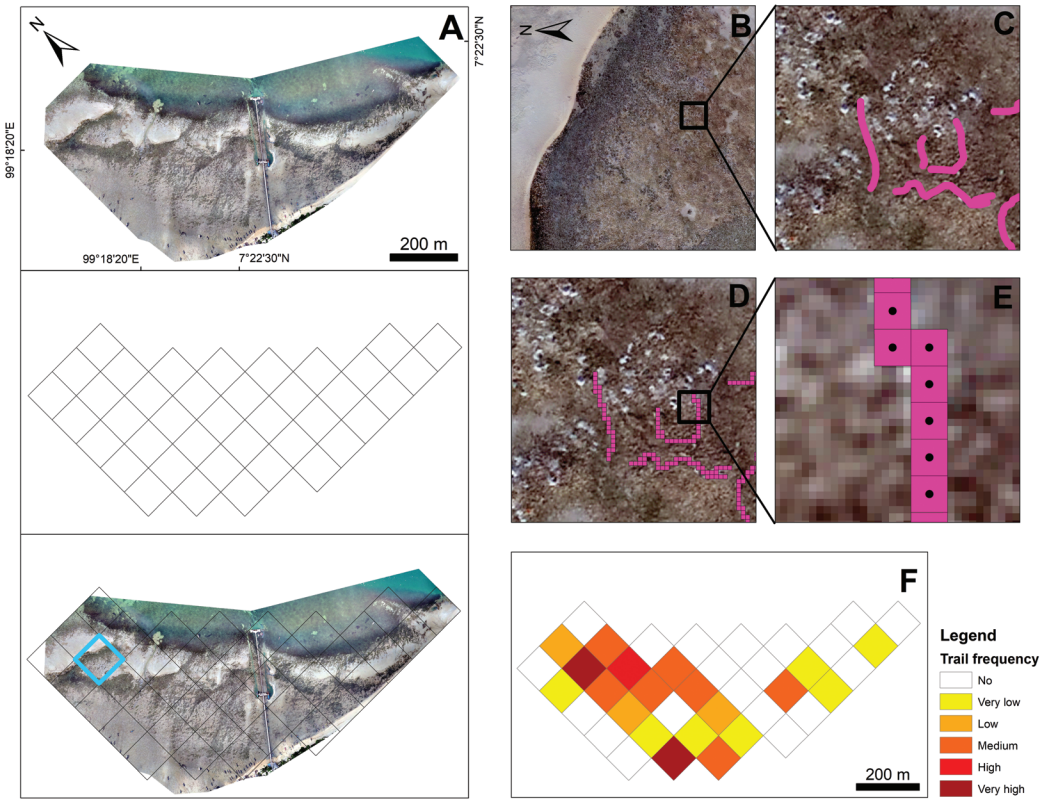

Figure 3. The identification of dugong feeding trails for temporal assessment involves the following steps: (A) an example of an RGB orthomosaic, a 100 × 100 m grid template, and the template applied to the mosaic, prepared for assessment (the blue square indicates the cell shown in B), (B) zooming into a 100 × 100 m grid cell, (C) further zooming into a 10 × 10 m grid cell and manually drawing lines along the dugong feeding trails (line layer), (D) creating points from the line layer and using the average trail width to set a point buffer, (E) zooming into a 1 × 1 m grid cell to show the points (black circles) and buffers (pink squares), and (F) joining the data from step D with the 100 × 100 m grid template, then displaying the quantities using color to represent values (count of points in each 100 × 100 m grid cell) with class interval.

feeding trails was used to create points utilizing the average trail width to set a point buffer (Figure 3D & E) and then joining the point data with the 100 × 100 m grid template and displaying the quantities using color to represent values (count of points in each 100 × 100 m grid cell) with class interval. The formula for class interval that was used to categorize the frequency of the trail can be expressed as follows:

$$\text{Class interval} = \frac{Max - Min}{Class} \quad (2)$$

where Max is the maximum value of the point count, Min is the minimum value of the point count, and Class is the number of categories of dugong feeding trail frequency. In this study, we divided the trail frequency into five classes: (1) very low, (2) low, (3) medium, (4) high, and (5) very high (Figure 3F).

Statistical analyses were performed using *R*, Version 4.4.0 for Windows (R Core Team, 2024). Data normality was assessed via the Shapiro–Wilk test ($\alpha = 0.05$), and homoscedasticity was assessed with Levene's test. Dugong feeding trail data, including the length, width, and area of the trails, were estimated following spatial assessment protocols. Length was log10 transformed for normality and variance homogeneity. Differences in trail width and length between months were compared using a one-way ANOVA, followed by Tukey's HSD test ($\alpha = 0.05$) for *post hoc* comparisons when significant variances were detected.

Processing of Seagrass Classification Maps

The seagrass classification was conducted on orthomosaics using RGB maps for the same three targeted sampling areas used in the spatial assessment study at three locations as explained: (1) Dugong Tower and (2) Juhoi on Libong Island, Trang, Thailand, and (3) Saco on Inhaca Island, Mozambique. The steps to create the seagrass distribution maps used to determine the area of seagrass and dugong trail distribution maps are depicted in Figure 4.

The seagrass boundaries were established in these targeted sampling areas by generating a spatial distribution map. The distribution of the seagrass was done using Maximum Likelihood Classification (MLC) with open-source software: 'SCP Plugin' for *QGIS*, Version 3.28.3 (QGIS Development Team, 2023). At each targeted sampling area, the collected ground data points were randomly divided into two groups of data points for the purpose of image classification training (70%) and validation of the classified images (30%). The image classification was done at the seagrass species level. Based on our targeted sampling area, five seagrass species were identified (*H. ovalis*, *C. rotundata*, *T. hemprichii*, *H. uninervis*, and *H. uninervis* mixed with *Z. capensis*); these were used as different classes together with three classes for barren substrate (rock, sand, and deep water). Since there was variability in the seagrass species composition, the number of seagrass classes varied from 2 to 3 in Thailand and 2 in Mozambique. Using both the resulting classification and reference data (validation data), an error matrix was constructed to calculate Overall Accuracy (OA), Producer's Accuracy (PA), User's Accuracy (UA), and the Kappa Coefficient (K), following the method described by Lillesand et al. (2015). OA indicates the general effectiveness of the classification process. The formula can be expressed as follows:

$$\mathrm{OA} = \frac{Number\ of\ correctly\ classified\ samples}{Total\ number\ of\ samples}\ x\ 100 \quad (3)$$

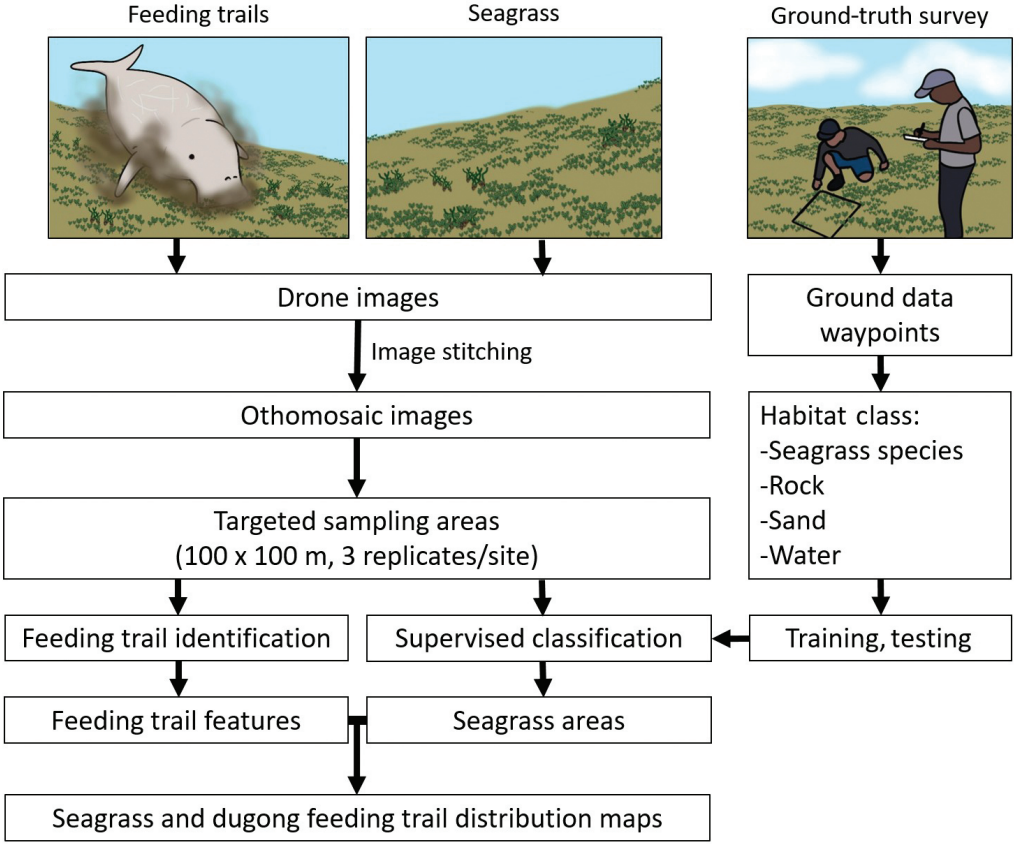

Figure 4. The processing for seagrass and dugong trail distribution maps

PA represents the likelihood that a certain land cover type on the ground-truth data (reference sample) is correctly classified in the map (omission error). The formula can be expressed as follows:

$$PA = \frac{Number\ of\ correctly\ classified\ samples\ for\ a\ class}{Total\ number\ of\ reference\ samples\ for\ that\ class}\ x\ 100 \quad (4)$$

UA refers to the probability that a class in the map accurately represents what is on the ground (commission error). The formula can be expressed as follows:

$$UA = \frac{Number\ of\ correctly\ classified\ samples\ for\ a\ class}{Total\ number\ of\ classified\ samples\ for\ that\ class}\ x\ 100 \quad (5)$$

K reflects the proportionate reduction in error achieved by the classification process compared to random classification. The K formula can be expressed as follows:

$$K = \frac{Po - Pe}{1 - Pe} \quad (6)$$

where Po represents observed agreement and is equivalent to OA but expressed as a decimal rather than a percentage (e.g., if OA is 85%, then Po = 0.85), and Pe represents expected agreement, calculated based on the distribution of samples across classes. K values range from -1 to +1. Higher values (K > 0.8) indicate strong agreement, moderate values (K = 0.4 to 0.8) reflect moderate agreement, and lower values (K < 0.4) suggest weak agreement.

Results

Comparison of RGB and NDVI Images

When detecting feeding trails, feeding trails were easy to detect in both RGB and NDVI images in denser vegetation patches (e.g., Juhoi). RGB effectively identified distinct trails, while NDVI highlighted the contrast between vegetated and non-vegetated areas (Figure 5). Additionally, there were no significant differences in trail measurements (count, length, or width) between RGB and NDVI images for Juhoi as shown in Table 2. In sparse areas (e.g., Dugong Tower and Saco), RGB images struggled due to visual complexity, while NDVI provided clearer detection by highlighting

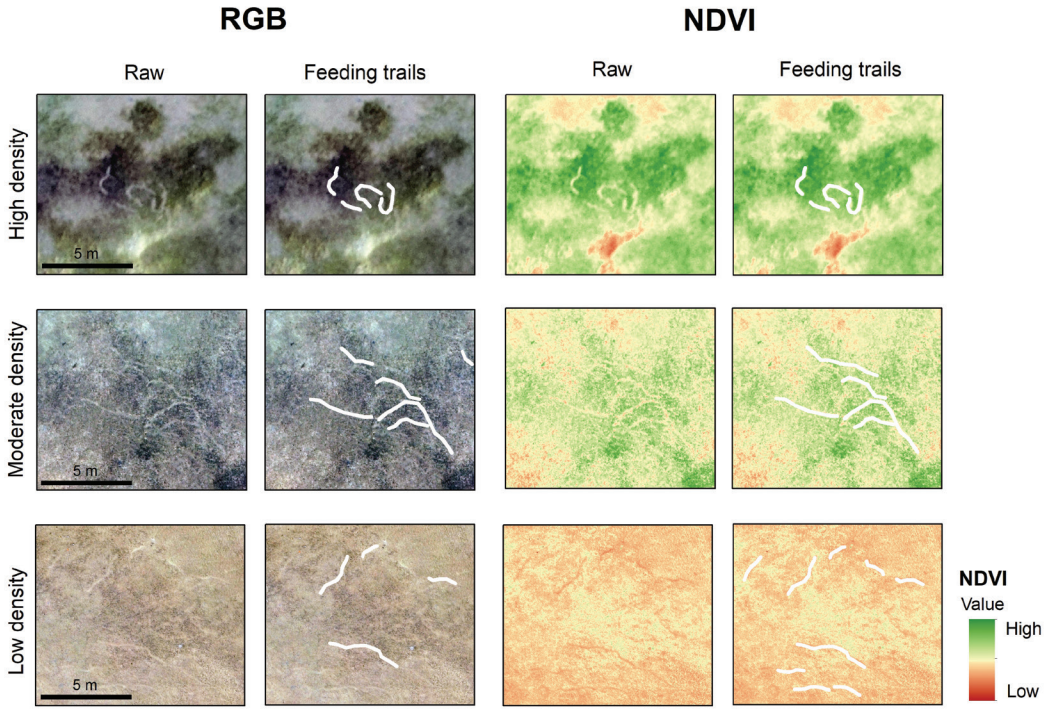

Figure 5. The variability of dugong feeding trails in RGB and NDVI images in different seagrass density levels. Note the same images are compared between the RGB and NDVI columns in each row.

Table 2. The mean, standard deviation (SD), and significance level (p value) of the comparisons in counts, lengths, and widths of dugong (*Dugong dugon*) feeding trails across RGB and NDVI images of each study site

	Count (no./ha)			Length (m)			Width (m)		
Site	RGB	NDVI	p value	RGB	NDVI	p value	RGB	NDVI	p value
Juhoi	721.33 ± 568.72	870.67 ± 55.18	0.67^{ns}	2.42 ± 1.50	1.94 ± 1.48	0.10^{ns}	0.24 ± 0.06	0.25 ± 0.05	0.66^{ns}
Dugong Tower	104.67 ± 87.07	69.67 ± 69.64	0.50^{ns}	3.17 ± 1.69	2.15 ± 1.03	0.32^{ns}	0.31 ± 0.10	0.32 ± 0.10	0.03*
Saco	935.67 ± 596.78	197.33 ± 150.19	0.11^{ns}	1.08 ± 0.61	2.39 ± 1.23	0.002**	0.15 ± 0.03	0.24 ± 0.05	0.0006***

Note: ns = nonsignificant differences, * = significant differences at $p < 0.05$, ** = significant differences at $p < 0.01$, and *** = significant differences at $p < 0.001$

vegetative contrasts (Figure 5). However, likely due to the difficulty in determining the trail boundary, significant differences in trail widths between RGB and NDVI images were observed for Dugong Tower and Saco as shown in Table 2.

UAV-Based Classification of Seagrass Orthophotos

The classification results provide a comprehensive evaluation of performance through several key metrics (Table 3). The classification achieved the Kappa Coefficient of 0.66, indicating moderate agreement between the classified data and ground-truth data. The OA of 92% represents a high proportion of correctly classified features. This high OA demonstrates the robustness of the classification method and suggests it is reliable for general analysis and mapping purposes. The PA of 90% indicates that 90% of the actual features on the ground were correctly identified in the classification, with a 10% omission error, meaning some ground-truth features were missing. Similarly, the UA of 90% reveals that 90% of the features classified as a certain class genuinely belonged to that class. The remaining 10% represent a commission error, where features were incorrectly assigned to that class. These metrics highlight the classifications' effectiveness in accurately identifying features, while the Kappa value suggests some room for improvement in distinguishing certain classes.

The accuracy of mapping varied across different habitat classes. Seagrass habitat was classified with high PA and UA accuracy (Table 3). The PA ranged from 83 to 100%, meaning that between 83 and 100% of the actual seagrass areas on the ground were correctly identified as seagrass in the classification. This suggests a relatively low omission error, with only a small proportion of seagrass areas being missed or misclassified. The UA ranging from 90 to 96% means that between 90 and 96% of the areas classified as seagrass in the map truly correspond to seagrass on the ground. This indicates a low commission error, with very few non-seagrass areas being misclassified as seagrass. For the sand habitat classification, the sand areas were identified correctly most of the time, although some misclassification occurred, mainly involving confusion with adjacent habitats such as sparse vegetation. The PA of 80% indicates that 80% of the actual sand habitat areas on the ground were correctly identified as sand in the classification. There is a 20% omission error, meaning that 20% of actual sand areas were not classified as sand. The UA of 90% indicates that 90% of the areas classified as sand in the map were actually sand on the ground. There is a 10% commission error, meaning some areas labeled as "sand" were misclassified and did not actually belong to the sand habitat. Despite the high PA of rock and water (100% of each class), only 57% of the areas mapped as rock and 41% of the areas mapped as water were correctly identified, as signified by the UA (Table 3).

Assessment of Dugong Feeding Trail Using UAVs: Spatial Maps

The availability of seagrass to the dugong varied across different sites. Among our targeted sampling areas, the average seagrass area in Juhoi, Dugong Tower, and Saco was 6,880.93 ± 777.91, 8,239.23 ± 197.50, and 7,652 ± 601.02 m^2, respectively. The highest density of dugong feeding trails in Juhoi was observed in *H. ovalis* patches. The area of dugong trails at Juhoi was 39.49 to 616.40 m^2 (0.61 to 10.38% of the sampling area). In Dugong Tower, the highest density of dugong feeding trails was observed in *C. rotundata* and *T. hemprichii* patches. The estimated area of dugong feeding trails in the area was 55.33 to 160.27 m^2 (0.70 to 1.77% of the sampling area). In

Table 3. Overall Accuracy (OA), Producer's Accuracy (PA), User's Accuracy (UA), and Kappa Coefficient (K) of the supervised classification for the targeted sampling areas

Sites		K	% accuracy		Seagrass					Sand	Rock	Deep water
			OA	Other	*Cr*	*Ho*	*Th*	*Hu*	*Hu* + *Zc*			
Juhoi	Area 1	0.86	99	PA	95	93	88	--	--	70	--	--
				UA	90	100	83	--	--	84	--	--
	Area 2	0.73	89	PA	97	76	--	--	--	97	--	--
				UA	76	100	--	--	--	70	--	--
	Area 3	0.79	90	PA	66	83	90	--	--	97	--	100
				UA	100	95	100	--	--	82	--	41
Dugong Tower	Area 1	0.59	90	PA	92	100	89	--	--	75	100	--
				UA	92	96	93	--	--	100	57	--
	Area 2	0.39	96	PA	--	89	95	--	--	92	--	--
				UA	--	91	90	--	--	95	--	--
	Area 3	0.56	96	PA	100	89	84	--	--	89	--	--
				UA	92	89	95	--	--	94	--	--
Saco	Area 1	0.53	86	PA	--	--	--	76	100	100	--	--
				UA	--	--	--	100	87	67	--	--
	Area 2	0.75	86	PA	--	--	--	78	100	100	--	--
				UA	--	--	--	100	100	63	--	--
	Area 3	0.73	92	PA	--	--	--	95	99	92	--	--
				UA	--	--	--	71	100	62	--	--
Average		0.66	92	PA	90	88	89	83	100	90	100	100
				UA	90	95	92	90	96	80	57	41

Note: *Cr* = *Cymodocea rotundata*, *Ho* = *Halophila ovalis*, *Th* = *Thalassia hemprichii*, *Hu* = *Halodule uninervis*, and *Hu* + *Zc* = *Halodule uninervis* mixed with *Zostera capensis*

Saco, the highest density of dugong feeding trails was observed in *H. uninervis* dominated patches. The estimated area of dugong feeding trails in the area was 49.32 to 300.39 m^2 (0.49 to 2.95% of the targeted sampling area) (Figure 6).

The statistical comparison of counts, lengths, and widths between RGB and NDVI images indicated no significant differences in counts across the study sites: Juhoi ($p = 0.67$), Dugong Tower ($p = 0.50$), and Saco ($p = 0.11$). The lengths showed significant differences only in Saco ($p = 0.002$), while the widths showed significant differences in Dugong Tower ($p = 0.03$) and highly significant differences in Saco ($p < 0.001$) (Table 2). From both RGB and NDVI images, the length of dugong feeding trails ranged from 10 to 1,337 no./ha^{-1}. The counts and widths ranged from 0.93 to 4.88 m and 0.14 to 0.37 m, respectively. The mean counts, lengths, and widths of dugong feeding trails derived from RGB and NDVI images across the three study sites are presented in Table 2. Notably, the highest count of feeding trails was recorded at Juhoi using the NDVI image (870.67 ± 55.18 no./ha), while the longest and widest trails were observed at Dugong Tower from the RGB image (3.17 ± 1.69 and 0.31 ± 0.10 m, respectively).

Temporal Variation in Feeding Activity at Mook Island

Two seagrass species were found to be dominant in the dugong feeding area at Mook Island, with

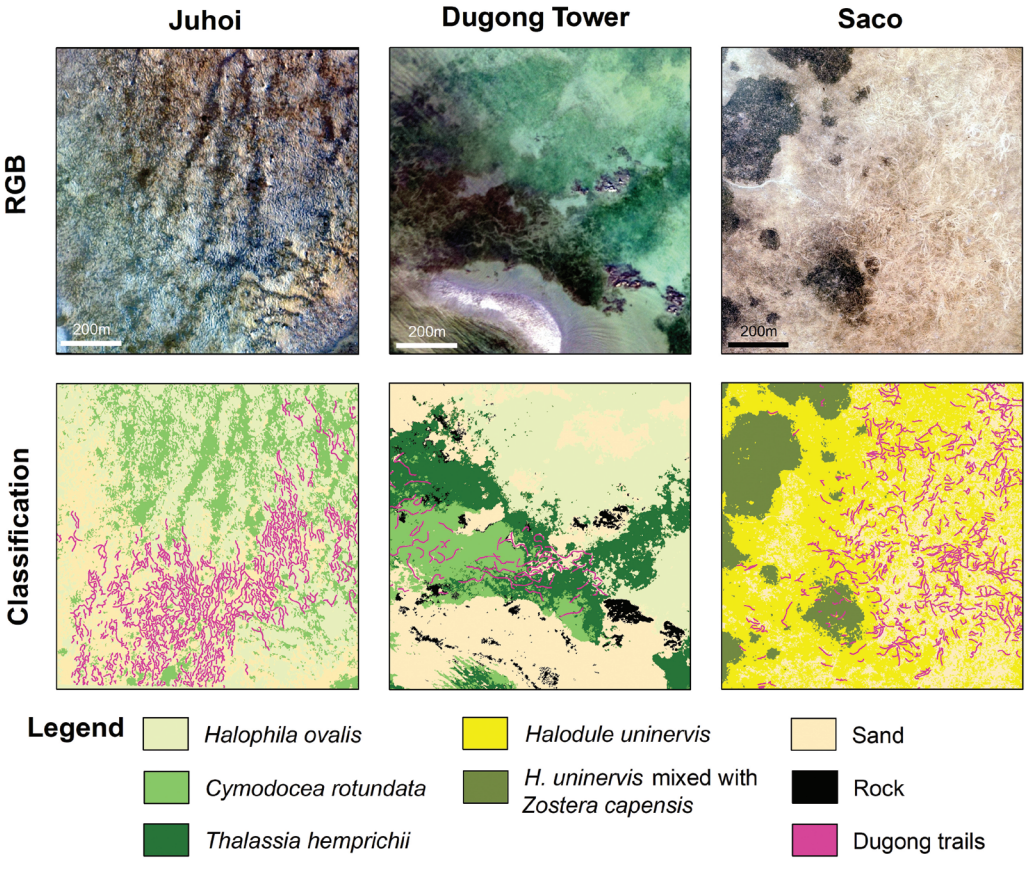

Figure 6. Example map of the seagrass species and sediment cover presented with dugong feeding trails from Juhoi, Dugong Tower, and Saco

H. ovalis being a dominant species in the area and showing high trail intensity and *H. pinifolia* being a nondominant species in the area but with many trails observed in their patches. The dugong feeding trails were distributed unevenly across the site, with the highest trail densities observed in specific areas during different survey dates (Figure 7). Feeding activity was consistently concentrated in the northwestern areas of the site (Figure 7B & F-H), suggesting habitual use of these locations by dugongs—in this case, dominated by *H. ovalis*. The highest trail density was observed in March to April 2021 (Figure 7G & H), corresponding to the dry season (December to April). Moreover, during April, dugong feeding trails covered the largest areas, indicating that feeding activity was more intense in the dry season. In contrast, trail density and area were lower during the wet season (May to November), especially in July and November 2020 (Figure 7B & D). Additionally, trail distribution patterns suggest a spatial structure in dugong foraging behavior. Certain months, such as July and November 2020 and February 2021 (Figure 7B, D & F), showed localized feeding with high-density trails in limited areas, while other months, such as April 2021 (Figure 7H), showed a broader spatial distribution. This may indicate variations in foraging strategies or seagrass regeneration patterns across different times of the year.

The number and area of feeding trails changed between the surveyed months at Mook Island. The highest number of feeding trails were observed in March 2021 (1,178 trails); while in other months, the number was much lower—at 11 to 488 trails (Figure 8A). In the dry season (from February to April 2021), the total area of dugong feeding trails was the largest (378.89 and 54.80 m^2, respectively); while in the wet season, the area of the feeding trail was low (13.88 to 45.88 m^2) (Figure 8B). The length and width of feeding trails also exhibited seasonal changes at Mook Island. The average length and width of feeding trails

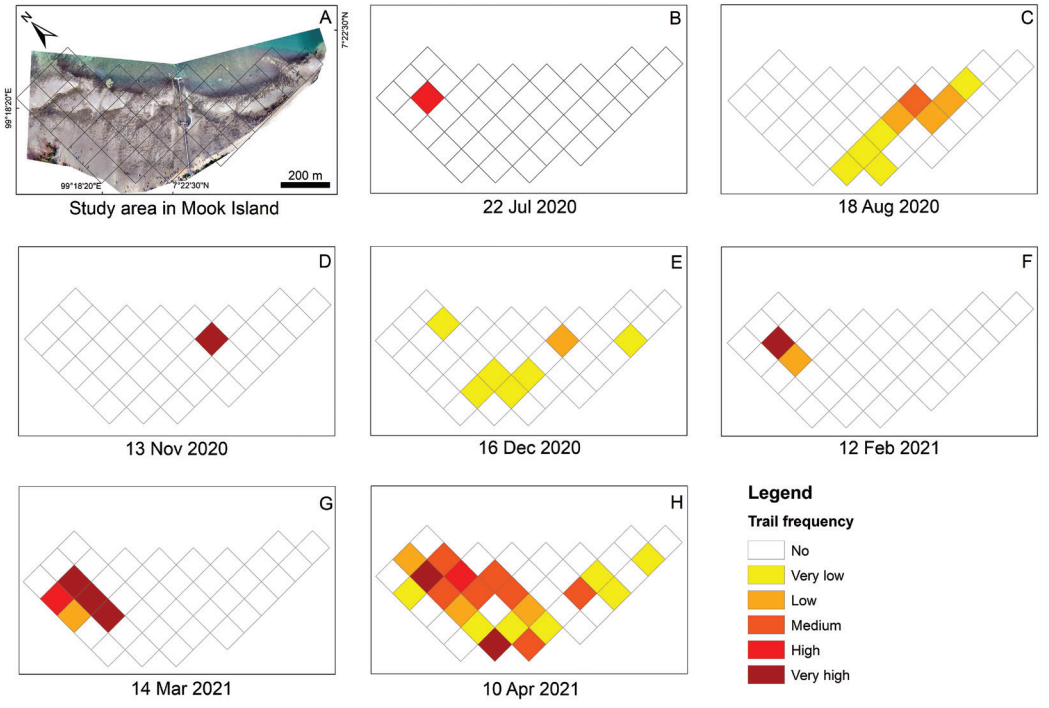

Figure 7. The distribution and density of dugong feeding trails (only dugong feeding trails that clearly occurred within seagrass meadows) at Mook Island on seven dates between July 2020 and April 2021

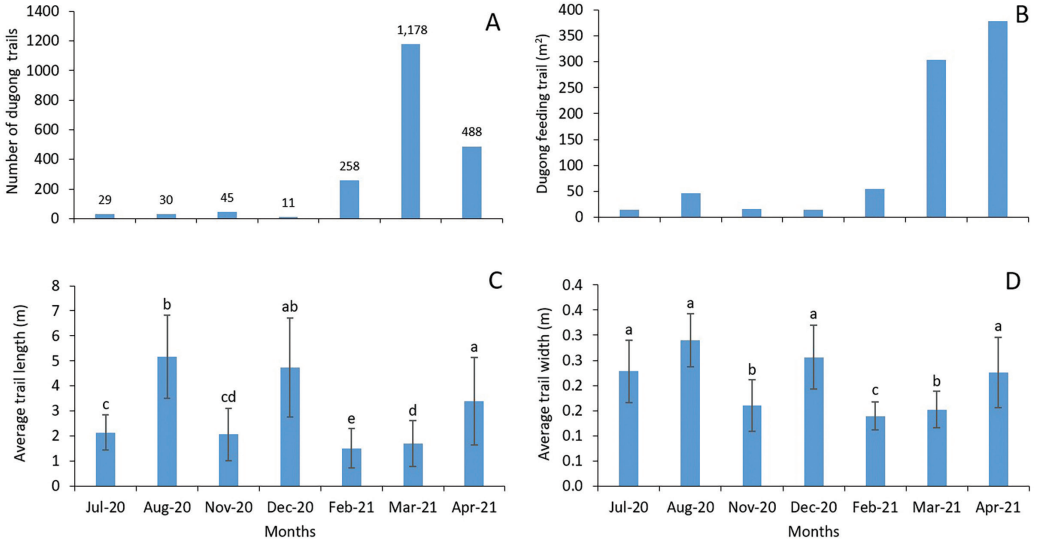

Figure 8. The summary of results of the dugong feeding trail analysis in the study site area at Mook Island during surveyed months: (A) total number of feeding trails, (B) total area covered by feeding trails (m^2), (C) average length of the feeding trails (m), and (D) average width of the feeding trails (m). Values with the same letter (lowercase letter in C and D) do not differ significantly between the months ($p < 0.05$; Tukey's HSD).

showed significant changes between the surveyed months ($p < 0.001$ for both). The average length was highest in August 2020, and the lowest average length was observed in February 2021 (mean ± SD: 5.17 ± 1.66 and 1.51 ± 0.78 m, respectively; Figure 8C). The average trail width was consistently high in July to August 2020, December 2020, and April 2021 (0.23 to 0.29 m), with the lowest points in November 2020 and February to March 2021 (0.14 to 0.16 m) (Figure 8D).

Discussion

UAV imagery can identify dugong feeding grounds at the scale of a meadow by analyzing trails within seagrass meadows. NDVI images (generated using multispectral cameras) exhibit higher consistency (lower SD) compared to RGB images to identify and measure dugong feeding trails, particularly in areas with low seagrass density (low NDVI values). UAV technology is adaptable to diverse geographic conditions, providing aerial perspectives of intertidal and coastal seagrass habitats. It facilitates the identification of critical feeding grounds and supports cross-regional comparisons, thereby informing global conservation strategies. Moreover, UAVs enable time-series data collection, allowing researchers to monitor changes in dugong activity, including shifts in habitat use. These insights are crucial for implementing effective management measures to protect seagrass meadows and ensure the long-term sustainability of this vulnerable marine species.

The Spatial and Temporal Monitoring of the Trails

This study demonstrates the high accuracy (92% on average) of UAVs in detecting seagrass species, seagrass areas, and dugong feeding grounds at a meadow scale. UAV imagery facilitates the spatial and temporal analysis of intertidal seagrass meadows and dugong feeding patterns. Spatial mapping, as highlighted by Riniatsih et al. (2021), utilizes UAV data to create detailed maps of seagrass distribution and species composition (Duffy et al., 2018a; Nahirnick et al., 2019; Hamad et al., 2022). Temporal mapping integrates time-dependent datasets to visualize changes, such as seasonal variations in seagrass habitats or patterns of dugong feeding trails (Roelfsema et al., 2014; Chayhard et al., 2018; Yamato et al., 2021; Cossa et al., 2023). Despite increased use of UAVs for seagrass monitoring (Nahirnick et al., 2019; James et al., 2020; Román et al., 2021; Price et al., 2022; B. Yang et al., 2023; Karang et al., 2024), there have been limited case studies on monitoring dugong feeding trails and small seagrass species like *H. ovalis* and *H. uninervis* (Yamato et al., 2021; Cossa et al., 2023), including this one.

Previous studies suggested that the availability of seagrass can be used to predict dugong presence by providing abundant food resources (Tol et al., 2016; Budiarsa et al., 2021; Heng et al., 2022). However, the availability alone does not confirm active foraging, which requires evidence such as grazing scars or excavations (Preen, 1995). Dugong foraging depends on factors like seagrass quality (e.g., nutritional content, species composition), higher density, and better accessibility (Sheppard et al., 2007; Marsh et al., 2011). In some locations, nutritional seagrass species (e.g., *H. ovalis* and *H. uninervis*), with high nitrogen and low indigestible fiber, are critical to dugong diets (Marsh et al., 1999; Sheppard et al., 2010), though dugongs are known to feed on all seagrass species (Erftemeijer et al., 1993; Adulyanukosol et al., 2004; Tol et al., 2016). However, dugongs may also forage in low-density meadows with preferred species (Sheppard et al., 2007; Marsh et al., 2011). Additionally, climatic factors, such as wind-driven wave generation and tidal fluctuations, may also affect feeding preferences (Budiarsa et al., 2021). Thus, while seagrass availability is an important ecological parameter, it is not a definitive predictor of dugong foraging behavior without corroborating evidence (Preen, 1995). However, a comprehensive understanding of dugong feeding preferences and foraging behavior is still lacking.

The temporal distribution of dugong feeding trails in Mook Island showed that the number of trails was low in the monsoon season. In the tropical region, monsoons strongly influence the seasons, and the possibility exists that wind speed, wind direction, and wave action may affect dugong migration and behavior (De Iongh et al., 2007; Sheppard et al., 2007). High wave action during monsoons can affect dugong navigation ability, which primarily relies on underwater sound (Burgess & Evans, 2022). Turbulent waves can disorient dugongs, making it challenging for them to locate and feed on seagrass beds. This disturbance may prompt changes in their feeding behavior or cause them to travel to calmer waters with more stable seagrass habitats (Budiarsa et al., 2021). Highlighting these several potential factors, we propose that our findings are limited to a local scale.

The measurements of feeding trails (number, length, and width) have important ecological and management implications, providing insights into dugong behavior, habitat use, and the impact of feeding on ecosystems. A higher number of trails may indicate a large dugong population and diverse feeding habits (Tol et al., 2016; Heng et al., 2022). Longer trails suggest extensive foraging activity and the availability of a large,

dispersed food supply (Preen, 1995; De Iongh et al., 2007). Trail width, roughly the width of a dugong's oral disk (Marshall et al., 2003), can reveal group structure, with most trails at our site likely made by adult dugongs, whose average trail width is between 0.17 and 0.30 m (Adulyanukosol et al., n.d.; Shawky, 2019). However, some trails exceeding 0.32 m have been observed in this study, indicating the presence of larger animals. In contrast, calves may leave trails ranging from 0.09 to 0.143 m wide (Adulyanukosol et al., n.d.; Tsutsumi et al., 2000).

Resource managers can use feeding trail data to design conservation areas and prioritize foraging zones (Ayad, 2021; Ng et al., 2022). Mannocci et al. (2024) recommend including areas with non-foraging activities, like dugong travel routes, in protected areas to safeguard seasonal movements. However, understanding foraging locations and intensity can guide ecotourism development, ensuring minimal impact on wildlife habitats (Ayad, 2021). Additionally, continuous monitoring of feeding trails provides long-term data on population and behavioral changes, informing conservation strategies and supporting sustainable wildlife management in response to environmental and climate changes.

The Methodologies and the Use of UAV Imagery for Seagrass and Dugong Feeding Trail Monitoring

Recent advancements in UAV-attached sensors, such as multispectral cameras, have enabled improved mapping of intertidal seagrass areas, becoming widely used to assess seagrass cover and biomass (James et al., 2020; Román et al., 2021). NDVI images are particularly valuable for identifying vegetation by visualizing vegetation health and density (Huang et al., 2021). While lightweight hyperspectral sensors for UAVs have been developed, their use remains limited due to complex pre- and post-flight analysis (Adão et al., 2017).

RGB images provide detailed plant characteristics, while NDVI images assess vegetation density, with higher values indicating denser vegetation. NDVI effectively detects spatial and temporal changes in seagrass ecosystems (Lyons et al., 2011; Roelfsema et al., 2014; Benmokhtar et al., 2023) and can be enhanced with color scales to measure vegetation health more precisely (Huang et al., 2021). When dugongs consume seagrass, they create feeding trails by uprooting plants. In this study, in denser areas (e.g., Juhoi), both RGB and NDVI effectively detected feeding trails, with RGB identifying distinct trails and NDVI highlighting contrasts. In sparse areas (e.g., Dugong Tower and Saco), NDVI provided clearer detection.

However, NDVI is sensitive to environmental factors like water transparency (C. Yang et al., 2010; Lu & Cho, 2011; Dierssen et al., 2019), which can affect its accuracy even at low tide when seagrass is exposed. Water in tidal pools or shallow areas can reduce light reflectance, leading to errors in NDVI values. To improve mapping accuracy, additional spectral bands and indices may be needed (Morgan et al., 2021). UAVs' high resolution enables detailed vegetation mapping and change detection, helping differentiate vegetation types and assess health (De Cock et al., 2023; B. Yang et al., 2023). Therefore, when monitoring seagrass and dugong feeding trails with UAVs, both image resolution and camera sensor specifications must be considered.

The Advantages and Limitations of the Use of UAVs for Seagrass and Dugong Feeding Trail Monitoring

UAVs are well-suited for monitoring dugong feeding trails and seagrass distribution on a local scale due to several key advantages. Their ability to navigate challenging locations allows access to remote areas, while automation and autonomous flight capabilities enhance data collection efficiency. UAVs are cost-effective compared to traditional methods, requiring less infrastructure and manpower; and they cause fewer disturbances to wildlife (Krause et al., 2021). With high-resolution imaging, UAVs enable detailed monitoring, such as tracking changes in seagrass abundance and distribution (Bernard et al., 2007). Additionally, UAVs can be equipped with various sensors to collect specific data, supporting applications like assessing marine ecosystem health and seagrass responses to stress (Aoki et al., 2022, 2023; B. Yang et al., 2023). Their versatility, cost-effectiveness, and efficiency make UAVs ideal for local-scale dugong feeding trail and seagrass monitoring.

While UAVs offer advantages for monitoring seagrass and dugongs, their adoption presents several challenges. Technical limitations, such as flight endurance, payload capacity, and sensor resolution, must be considered. Data processing challenges include managing large volumes of imagery, ensuring data accuracy, and integrating findings for conservation management. Environmental factors like water levels, turbidity, and sun glint can affect image quality, while adverse weather conditions, such as rain and strong winds, can hinder UAV flights and compromise data collection (Hodgson et al., 2013; B. Yang et al., 2023).

Conclusions

This study demonstrates the use of UAVs to detect seagrass distribution and dugong feeding grounds in intertidal seagrass meadows. We also provided examples of seagrass classification schemes. Additionally, we combined aerial survey data with ground surveys to obtain spatial information on seagrass areas and the distribution of dugong feeding trails in three geographically diverse locations: (1) Juhoi and (2) Dugong Tower, Libong Island, Thailand, and (3) Saco, Inhaca Island, Mozambique, as well as the temporal distribution of dugong feeding trails on Mook Island, Thailand. While UAVs provide valuable data for monitoring seagrass and dugong feeding areas, challenges such as restricted flight endurance and adverse weather conditions can limit their suitability for environmental monitoring in certain situations.

To address challenges in UAV-based environmental monitoring, advancements in technology, regulatory frameworks, and operations continue to expand their application. Combining UAV technology with dugong feeding trail monitoring improves our ability to study and protect dugongs and their seagrass habitats. The integration of advanced sensors, machine learning, and remote sensing offers a comprehensive approach to ecological research and conservation. Additionally, expertise in seagrass and dugong biology, along with data analysis skills, is crucial for accurately processing and interpreting the data.

Further research into integrating machine learning with UAV data can improve the identification of dugong feeding trails by automating image analysis and recognizing foraging patterns. Incorporating bathymetric data, time-series maps, and extensive UAV surveys can enhance the accuracy of seagrass dynamics estimations, aiding effective conservation and management.

Note: The supplemental figures for this article are available in the "Supplemental Material" section of the *Aquatic Mammals* website: https://www.aquaticmammalsjournal.org/supplemental-material.

Acknowledgments

This work was supported by the Faculty of Science Research Fund, Prince of Songkla University, Contract No. 1-2563-02-002. The authors are thankful to the team members and interns from the Seaweed and Seagrass Research Unit, Faculty of Science, Prince of Songkla University, for their valuable time spent on data analysis and for suggestions on the manuscript. Field data collection was financially supported by PSU–TUYF under the Seagrass and Dugong Project.

Literature Cited

Adão, T., Hruška, J., Pádua, L., Bessa, J., Peres, E., Morais, R., & Sousa, J. J. (2017). Hyperspectral imaging: A review on UAV-based sensors, data processing and applications for agriculture and forestry. *Remote Sensing*, *9*(11), 1110. https://doi.org/10.3390/rs9111110

Adulyanukosol, K., Boukaew, P., & Prasitthipornkul, A. (2004, December). Analysis of stomach contents of dugongs (*Dugong dugon*) from Gulf of Thailand. *Proceedings of the International Symposium on SEASTAR2000 and Bio-Logging Science* (The 5th SEASTAR2000 Workshop, pp. 45-51), Bangkok, Thailand.

Adulyanukosol, K., Thongsukdee, S., & Poovachiranon, S. (n.d.). *An observation of dugong behaviors from aerial surveys and feeding trails of a cow–calf pair in seagrass habitat*. Department of Marine and Coastal Resources, Ministry of Natural Resources and Environment, Thailand.

Aoki, L., Yang, B., Graham, O., Gomes, C., Rappazzo, B., Hawthorne, T., Duffy, E., & Harvell, D. (2023). UAV high-resolution imaging and disease surveys combine to quantify climate-related decline in seagrass meadows. *Oceanography*, *36*(1), 38-39. https://doi.org/10.5670/oceanog.2023.s1.12

Aoki, L. R., Rappazzo, B., Beatty, D. S., Domke, L. K., Eckert, G. L., Eisenlord, M. E., Graham, O. J., Harper, L., Hawthorne, T. L., Hessing-Lewis, M., Hovel, K. A., Monteith, Z. L., Mueller, R. S., Olson, A. M., Prentice, C., Stachowicz, J. J., Tomas, F., Yang, B., Duffy, J. E., & Harvell, C. D. (2022). Disease surveillance by artificial intelligence links eelgrass wasting disease to ocean warming across latitudes. *Limnology and Oceanography*, *67*(7), 1577-1589. https://doi.org/10.1002/lno.12152

Ayad, T. H. (2021). Dugong based tourism development at the Red Sea: Case of Marsa Abu Dabab. *African Journal of Hospitality, Tourism and Leisure*, *10*(2), 608-622. https://doi.org/10.46222/ajhtl.19770720-121

Bandeira, S., & Gullström, M. (2014). Seagrass meadows in Maputo Bay. In S. Bandeira & J. Paula (Eds.), *The Maputo Bay ecosystem* (pp. 147-186). WIOMSA, Zanzibar Town. 427 pp.

Benmokhtar, S., Robin, M., Maanan, M., Boutoumit, S., Badaoui, B., & Bazairi, H. (2023). Monitoring the spatial and interannual dynamic of *Zostera noltei*. *Wetlands*, *43*(5), 1-16. https://doi.org/10.1007/s13157-023-01690-7

Bernard, G., Boudouresque, C. F., & Picon, P. (2007). Long term changes in *Zostera* meadows in the Berre Lagoon (Provence, Mediterranean Sea). *Estuarine, Coastal and Shelf Science*, *73*(3-4), 617-629. https://doi.org/10.1016/j.ecss.2007.03.003

Budiarsa, A. A., De Iongh, H. H., Kustiawan, W., & van Bodegom, P. M. (2021). Dugong foraging behavior on tropical intertidal seagrass meadows: The influence of climatic drivers and anthropogenic disturbance. *Hydrobiologia*, *848*(18), 4153-4166. https://doi.org/10.1007/s10750-021-04583-0

Burgess, M., & Evans, K. O. (2022). Sirenia navigation. In J. Vonk & T. K. Shackelford (Eds.), *Encyclopedia of*

animal cognition and behavior (pp. 6446-6451). Springer International Publishing. https://doi.org/10.1007/978-3-319-55065-7_1332

Carroll, D., Infantes, E., Pagan, E., & Hardin, K. (2024). Approaching a population-level assessment of body size in pinnipeds using drones, an early warning of environmental degradation. *Remote Sensing in Ecology and Conservation*, *11*(2), 156-171. https://doi.org/10.1002/rse2.413

Chayhard, S., Manthachitra, V., Nualchawee, K., & Buranaprathepat, A. (2018). Multi temporal mapping of seagrass distribution by using integrated remote sensing data in Kung Kraben Bay (KKB), Chanthaburi Province, Thailand. *International Journal of Agricultural Technology*, *14*(2), 161-170.

Chen, J-J., Zhen, S., & Sun, Y. (2021). Estimating leaf chlorophyll content of buffalo berry using normalized difference vegetation index sensors. *HortTechnology*, *31*(3), 297-303. https://doi.org/10.21273/HORTTECH04808–21

Cleguer, C., Kelly, N., Tyne, J., Wieser, M., Peel, D., & Hodgson, A. (2021). A novel method for using small unoccupied aerial vehicles to survey wildlife species and model their density distribution. *Frontiers in Marine Science*, *8*, 640338. https://doi.org/10.3389/fmars.2021.640338

Cossa, D., Cossa, M., Timba, I., Nhaca, J., Macia, A., & Infantes, E. (2023). Drones and machine-learning for monitoring dugong feeding grounds and gillnet fishing. *Marine Ecology Progress Series*, *716*, 123-136. https://doi.org/10.3354/MEPS14361

De Cock, A., Vandeputte, R., Bruneel, S., De Cock, L., Liu, X., Bermúdez, R., Vanhaeren, N., De Wit, B., Ochoa, D., De Maeyer, P., Gautama, S., & Goethals, P. L. M. (2023). Construction of an orthophoto-draped 3D model and classification of intertidal habitats using UAV imagery in the Galapagos Archipelago. *Drones*, *7*(7), 416. https://doi.org/10.3390/DRONES7070416

De Iongh, H. H., Kiswara, A. W., Kustiawan, A. W., & Loth, A. P. E. (2007). A review of research on the interactions between dugongs (*Dugong dugon* Müller 1776) and intertidal seagrass beds in Indonesia. *Hydrobiologia*, *591*, 73-83. https://doi.org/10.1007/s10750-007-0785-4

Dierssen, H. M., Bostrom, K. J., Chlus, A., Hammerstrom, K., Thompson, D. R., & Lee, Z. (2019). Pushing the limits of seagrass remote sensing in the turbid waters of Elkhorn Slough, California. *Remote Sensing*, *11*(14), 1664. https://doi.org/10.3390/rs11141664

Duffy, J. P., Pratt, L., Anderson, K., Land, P. E., & Shutler, J. D. (2018a). Spatial assessment of intertidal seagrass meadows using optical imaging systems and a lightweight drone. *Estuarine, Coastal and Shelf Science*, *200*, 169-180. https://doi.org/10.1016/j.ecss.2017.11.001

Duffy, J. P., Cunliffe, A. M., DeBell, L., Sandbrook, C., Wich, S. A., Shutler, J. D., Myers Smith, I. H., Varela, M. R., & Anderson, K. (2018b). Location, location, location: Considerations when using lightweight drones in challenging environments. *Remote Sensing in Ecology and Conservation*, *4*(1), 7-19. https://doi.org/10.1002/rse2.58

Erftemeijer, P. L. A., Djunarlin, & Moka, W. (1993). Stomach content analysis of a dugong (*Dugong dugon*) from south Sulawesi, Indonesia. *Marine and Freshwater Research*, *44*(1), 229-233. https://doi.org/10.1071/MF9930229

Hamad, I. Y., Staehr, P. A. U., Rasmussen, M. B., & Sheikh, M. (2022). Drone-based characterization of seagrass habitats in the tropical waters of Zanzibar. *Remote Sensing*, *14*(3), 680. https://doi.org/10.3390/rs14030680

Heng, H. W. K., Ooi, J. L. S., Affendi, Y. A., Kee Alfian, A. A., & Ponnampalam, L. S. (2022). Dugong feeding grounds and spatial feeding patterns in subtidal seagrass: A case study at Sibu Archipelago, Malaysia. *Estuarine, Coastal and Shelf Science*, *264*, 107670. https://doi.org/10.1016/j.ecss.2021.107670

Hodgson, A., Kelly, N., & Peel, D. (2013). Unmanned aerial vehicles (UAVs) for surveying marine fauna: A dugong case study. *PLOS One*, *8*(11), e79556. https://doi.org/10.1371/journal.pone.0079556

Huang, S., Tang, L., Hupy, J. P., Wang, Y., & Shao, G. (2021). A commentary review on the use of normalized difference vegetation index (NDVI) in the era of popular remote sensing. *Journal of Forestry Research*, *32*(1), 1-6. https://doi.org/10.1007/s11676-020-01155-1

Infantes, E., Carroll, D., Silva, W. T. A. F., Härkönen, T., Edwards, S. V., & Harding, K. C. (2022). An automated work-flow for pinniped surveys: A new tool for monitoring population dynamics. *Frontiers in Ecology and Evolution*, *10*, 905309. https://doi.org/10.3389/fevo.2022.905309

Infantes, E., Cossa, D., Stankovic, M., Panyawai, J., Tuntiprapas, P., Daochai, C., & Prathep, A. (2020). Dugong (*Dugong dugon*) reproductive behaviour in Koh Libong, Thailand: Observations using drones. *Aquatic Mammals*, *46*(6), 603-608. https://doi.org/10.1578/AM.46.6.2020.603

James, D., Collin, A., Houet, T., Mury, A., Gloria, H., & Le Poulain, N. (2020). Towards better mapping of seagrass meadows using UAV multispectral and topographic data. *Journal of Coastal Research*, *95*(SI), 1117-1121. https://doi.org/10.2112/SI95-217.1

Karang, I. W. G. A., Pravitha, N. L. P. R., Nuarsa, I. W., Ahammed, K. K. B., & Wicaksono, P. (2024). High-resolution seagrass species mapping and propeller scars detection in Tanjung Benoa, Bali through UAV imagery. *Journal of Ecological Engineering*, *25*(1), 161-174. https://doi.org/10.12911/22998993/174943

Kilminster, K., McMahon, K., Waycott, M., Kendrick, G. A., Scanes, P., McKenzie, L., O'Brien, K. R., Lyons, M., Ferguson, A., Maxwell, P., Glasby, T., & Udy, J. (2015). Unravelling complexity in seagrass systems for management: Australia as a microcosm. *Science of the Total Environment*, *534*, 97-109. https://doi.org/10.1016/j.scitotenv.2015.04.061

Krause, D. J., Hinke, J. T., Goebel, M. E., & Perryman, W. L. (2021). Drones minimize Antarctic predator responses relative to ground survey methods: An appeal for context in policy advice. *Frontiers in Marine Science*, *8*, 1-15. https://doi.org/10.3389/fmars.2021.648772

Li, Y., Bai, J., Chen, S., Chen, B., & Zhang, L. (2023). Mapping seagrasses on the basis of Sentinel-2 images under tidal

change. *Marine Environmental Research*, *185*, 105880. https://doi.org/10.1016/j.marenvres.2023.105880

Lillesand, T. M., Kiefer, R. W., & Chipman, J. W. (2015). *Remote sensing and image interpretation* (7th ed.). Wiley.

Lu, D., & Cho, H. J. (2011). An improved water-depth correction algorithm for seagrass mapping using hyperspectral data. *Remote Sensing Letters*, *2*(2), 91-97. https://doi.org/10.1080/01431161.2010.502152

Lyons, M., Phinn, S., & Roelfsema, C. (2011). Integrating quickbird multi-spectral satellite and field data: Mapping bathymetry, seagrass cover, seagrass species and change in Moreton Bay, Australia in 2004 and 2007. *Remote Sensing*, *3*(1), 42-64. https://doi.org/10.3390/rs3010042

Mannocci, L., Derville, S., Seguin, R., & Mouillot, D. (2024). Aerial video surveys and spatial prioritization reveal conservation opportunities for endangered dugongs in New Caledonia. *Aquatic Conservation: Marine and Freshwater Ecosystems*, *34*(8), e4237. https://doi.org/10.1002/aqc.4237

Marsh, H., O'Shea, T. J., & Reynolds III, J. E. (2011). *Ecology and conservation of the Sirenia: Dugongs and manatees*. Cambridge University Press. https://doi.org/10.1017/CBO9781139013277

Marsh, H., Eros, C., Corkeron, P., & Breen, B. (1999). A conservation strategy for dugongs: Implications of Australian research. *Marine and Freshwater Research*, *50*(8), 979-990. https://doi.org/10.1071/MF99080

Marshall, C. D., Maeda, H., Iwata, M., Furuta, M., Asano, S., Rosas, F., & Reep, R. L. (2003). Orofacial morphology and feeding behaviour of the dugong, Amazonian, West African and Antillean manatees (Mammalia: Sirenia): Functional morphology of the muscular vibrissal complex. *Journal of Zoology*, *259*(3), 245-260. https://doi.org/10.1017/S0952836902003205

McKenzie, L. J., Campbell, S. J., & Roder, C. A. (2006). *Seagrass-Watch: Manual for mapping & monitoring seagrass resources by community (citizen) volunteers*. QFS, NFC, Cairns.

Morgan, G. R., Wang, C., & Morris, J. T. (2021). RGB indices and canopy height modelling for mapping tidal marsh biomass from a small unmanned aerial system. *Remote Sensing*, *13*(17), 3406. https://doi.org/10.3390/rs13173406

Murfitt, S. L., Allan, B. M., Bellgrove, A., Rattray, A., Young, M. A., & Ierodiaconou, D. (2017). Applications of unmanned aerial vehicles in intertidal reef monitoring. *Scientific Reports*, *7*(1), 10259. https://doi.org/10.1038/s41598-017-10818-9

Nababan, B., Mastu, L. O. K., Idris, N. H., & Panjaitan, J. P. (2021). Shallow-water benthic habitat mapping using drone with object based image analyses. *Remote Sensing*, *13*(21), 4452. https://doi.org/10.3390/rs13214452

Nahirnick, N. K., Reshitnyk, L., Campbell, M., Hessing-Lewis, M., Costa, M., Yakimishyn, J., & Lee, L. (2019). Mapping with confidence; delineating seagrass habitats using unoccupied aerial systems (UAS). *Remote Sensing in Ecology and Conservation*, *5*(2), 121-135. https://doi.org/10.1002/rse2.98

Nakaoka, M., & Aioi, K. (1999). Growth of seagrass *Halophila ovalis* at dugong trails compared to existing within-patch variation in a Thailand intertidal flat. *Marine Ecology Progress Series*, *184*, 97-103. https://doi.org/10.3354/meps184097

Ng, S. Z. H., Ow, Y. X., & Jaafar, Z. (2022). Dugongs (*Dugong dugon*) along hyper-urbanized coastlines. *Frontiers in Marine Science*, *9*, 1799. https://doi.org/10.3389/fmars.2022.947700

Preen, A. (1995). Impacts of dugong foraging on seagrass habitats: Observational and experimental evidence for cultivation grazing. *Marine Ecology Progress Series*, *124*(1-3), 201-213. https://doi.org/10.3354/meps124201

Price, D. M., Felgate, S. L., Huvenne, V. A. I., Strong, J., Carpenter, S., Barry, C., Lichtschlag, A., Sanders, R., Carrias, A., Young, A., Andrade, V., Cobb, E., Le Bas, T., Brittain, H., & Evans, C. (2022). Quantifying the intra-habitat variation of seagrass beds with unoccupied aerial vehicles (UAVs). *Remote Sensing*, *14*(3), 480. https://doi.org/10.3390/RS14030480

QGIS Development Team. (2023). *QGIS geographic information system*. Open Source Geospatial Foundation Project. http://qgis.osgeo.org

R Core Team. (2024). R*: A language and environment for statistical computing*. R Foundation for Statistical Computing. https://www.Rproject.org

Ramos, E. A., Landeo-Yauri, S., Castelblanco-Martínez, N., Arreola, M. R., Quade, A. H., & Rieucau, G. (2022). Drone-based photogrammetry assessments of body size and body condition of Antillean manatees. *Mammalian Biology*, *102*(3), 765-779. https://doi.org/10.1007/s42991-022-00228-4

Raoult, V., Colefax, A. P., Allan, B. M., Cagnazzi, D., Castelblanco-Martínez, N., Ierodiaconou, D., Johnston, D. W., Landeo-Yauri, S., Lyons, M., Pirotta, V., Schofield, G., & Butcher, P. A. (2020). Operational protocols for the use of drones in marine animal research. *Drones*, *4*(4), 64. https://doi.org/10.3390/drones4040064

Riniatsih, I., Ambariyanto, A., Yudiati, E., Redjeki, S., Hartati, R., Triaji, R. M. J., & Siagian, H. (2021). Spatial assessment of seagrass ecosystem using the unmanned aerial vehicle (UAV) in Teluk Awur, coastal water of Jepara. *IOP Conference Series: Earth and Environmental Science*, *744*(1). https://doi.org/10.1088/1755-1315/744/1/012063

Roelfsema, C. M., Lyons, M., Kovacs, E. M., Maxwell, P., Saunders, M. I., Samper-Villarreal, J., & Phinn, S. R. (2014). Multi-temporal mapping of seagrass cover, species and biomass: A semi-automated object based image analysis approach. *Remote Sensing of Environment*, *150*, 172-187. https://doi.org/10.1016/j.rse.2014.05.001

Román, A., Tovar-Sánchez, A., Olivé, I., & Navarro, G. (2021). Using a UAV-mounted multispectral camera for the monitoring of marine macrophytes. *Frontiers in Marine Science*, *8*, 722698. https://doi.org/10.3389/fmars.2021.722698

Ryan, K. P., Ferguson, S. H., Koski, W. R., Young, B. G., Roth, J. D., & Watt, C. A. (2022). Use of drones for the creation and development of a photographic identification catalogue for an endangered whale population. *Arctic Science*, *8*(4), 1191-1201. https://doi.org/10.1139/as-2021-0047

Schofield, G., Esteban, N., Katselidis, K. A., & Hays, G. C. (2019). Drones for research on sea turtles and other marine vertebrates—A review. *Biological Conservation*, *238*, 108214. https://doi.org/10.1016/j.biocon.2019.108214

Shawky, A. M. (2019). Evidence of the occurrence of a large dugong in the Red Sea, Egypt. *Egyptian Journal of Aquatic Research*, *45*(3), 247-250. https://doi.org/10.1016/j.ejar.2019.08.001

Sheppard, J. K., Lawler, I. R., & Marsh, H. (2007). Seagrass as pasture for seacows: Landscape-level dugong habitat evaluation. *Estuarine, Coastal and Shelf Science*, *71*(1-2), 117-132. https://doi.org/10.1016/j.ecss.2006.07.006

Sheppard, J. K., Marsh, H., Jones, R. E., & Lawler, I. R. (2010). Dugong habitat use in relation to seagrass nutrients, tides, and diel cycles. *Marine Mammal Science*, *26*(4), 855-879. https://doi.org/10.1111/j.1748-7692.2010.00374.x

Tahara, S., Sudo, K., Yamakita, T., & Nakaoka, M. (2022). Species level mapping of a seagrass bed using an unmanned aerial vehicle and deep learning technique. *PeerJ*, *10*, e14017. https://doi.org/10.7717/peerj.14017/supp-2

Tol, S. J., Coles, R. G., & Congdon, B. C. (2016). *Dugong dugon* feeding in tropical Australian seagrass meadows: Implications for conservation planning. *PeerJ*, *4*, e2194. https://doi.org/10.7717/peerj.2194

Trinh, X. T., Nguyen, L. D., & Takeuchi, W. (2023). Sentinel-2 mapping of a turbid intertidal seagrass meadow in southern Vietnam. *Geocarto International*, *38*(1). https://doi.org/10.1080/10106049.2023.2186490

Tsutsumi, C., Ichikawa, K., Akamatsu, T., Arai, N., Shinke, T., & Hara, T. (2000, December). Monitoring dugong feeding behavior in a tidal flat by visual and acoustic observation. *Proceedings of the 2nd International Symposium on SEASTAR2000 and Asian Bio-Logging Science* (The 6th SEASTAR2000 Workshop, pp. 37-42), Bangkok, Thailand.

Yamamuro, M., & Chirapart, A. (2005). Quality of the seagrass *Halophila ovalis* on a Thai intertidal flat as food for the dugong. *Journal of Oceanography*, *61*, 183-186. https://doi.org/10.1007/s10872-005-0030-6

Yamato, C., Ichikawa, K., Arai, N., Tanaka, K., Nishiyama, T., & Kittiwattanawong, K. (2021). Deep neural networks based automated extraction of dugong feeding trails from UAV images in the intertidal seagrass beds. *PLOS One*, *16*(8), e0255586. https://doi.org/10.1371/journal.pone.0255586

Yang, B., Hawthorne, T. L., Aoki, L., Beatty, D. S., Copeland, T., Domke, L. K., Eckert, G. L., Gomes, C. P., Graham, O. J., Harvell, C. D., Hovel, K. A., Hessing-Lewis, M., Harper, L., Mueller, R. S., Rappazzo, B., Reshitnyk, L., Stachowicz, J. J., Tomas, F., & Duffy, J. E. (2023). Low-altitude UAV imaging accurately quantifies eelgrass wasting disease from Alaska to California. *Geophysical Research Letters*, *50*(4), e2022GL101985. https://doi.org/10.1029/2022GL101985

Yang, C., Yang, D., Cao, W., Zhao, J., Wang, G., Sun, Z., Xu, Z., & Ravi Kumar, M. S. (2010). Analysis of seagrass reflectivity by using a water column correction algorithm. *International Journal of Remote Sensing*, *31*(17), 4595-4608. https://doi.org/10.1080/01431161.2010.485138